

Small Angle X-ray Scattering (SAXS) and Biological Applications

Zehra Sayers
Sabanci University, Istanbul, Turkey
SESAME, Chair, Scientific Advisory Committee

Overview

- Protein folding and structure.
- Principles of Small Angle X-ray Scattering (SAXS).
- SAXS measurements on biological samples.
- Ab initio* modeling
 - Heterotrimeric G-proteins of *A. Thaliana*
 - Metallothioneins from wheat.

Levels of Protein Folding

Primary structure: **Linear** amino acid sequence; directional.

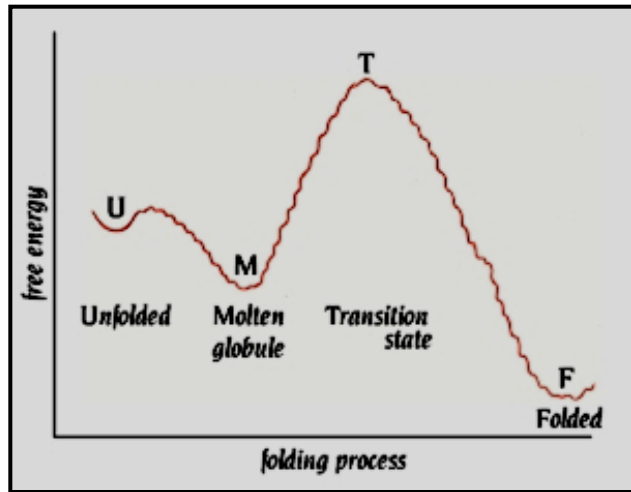
N-Terminal → MSVELKERHAVA..... KIWAFGGHRRVI → **C-Terminal**

Secondary structure: Regions with defined fold;
alpha helices and beta sheets

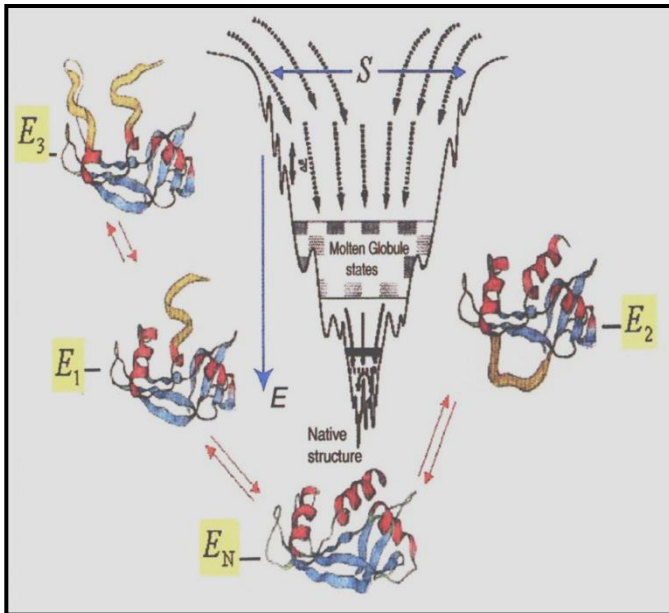
Tertiary structure: **Fully folded 3D molecular structure** of a single chain.

Quaternary structure: 3D structure of a **multi-chain** molecule.

Protein Folding

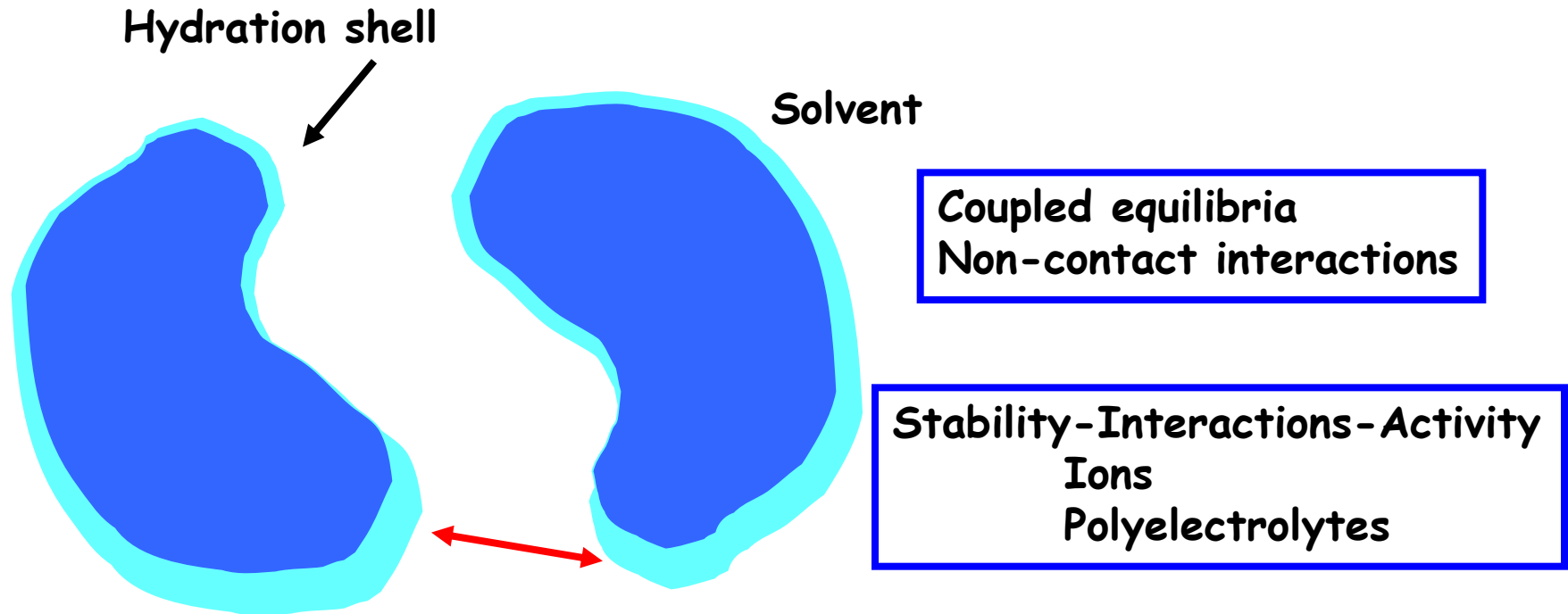


Folding process: transition from the high-energy unfolded state to low energy folded state.



A number of metastable intermediate states are sampled before folded state is reached.
In solution there may be a dynamic equilibrium of different conformations.

Protein Structure in Solution



Protein crowding in cells:
Maximum concentration 300-500mg/ml.

Macromolecular Structure Determination

X-ray Crystallography

Snapshots of the 3D structure at atomic resolution.
Static measurements*

NMR

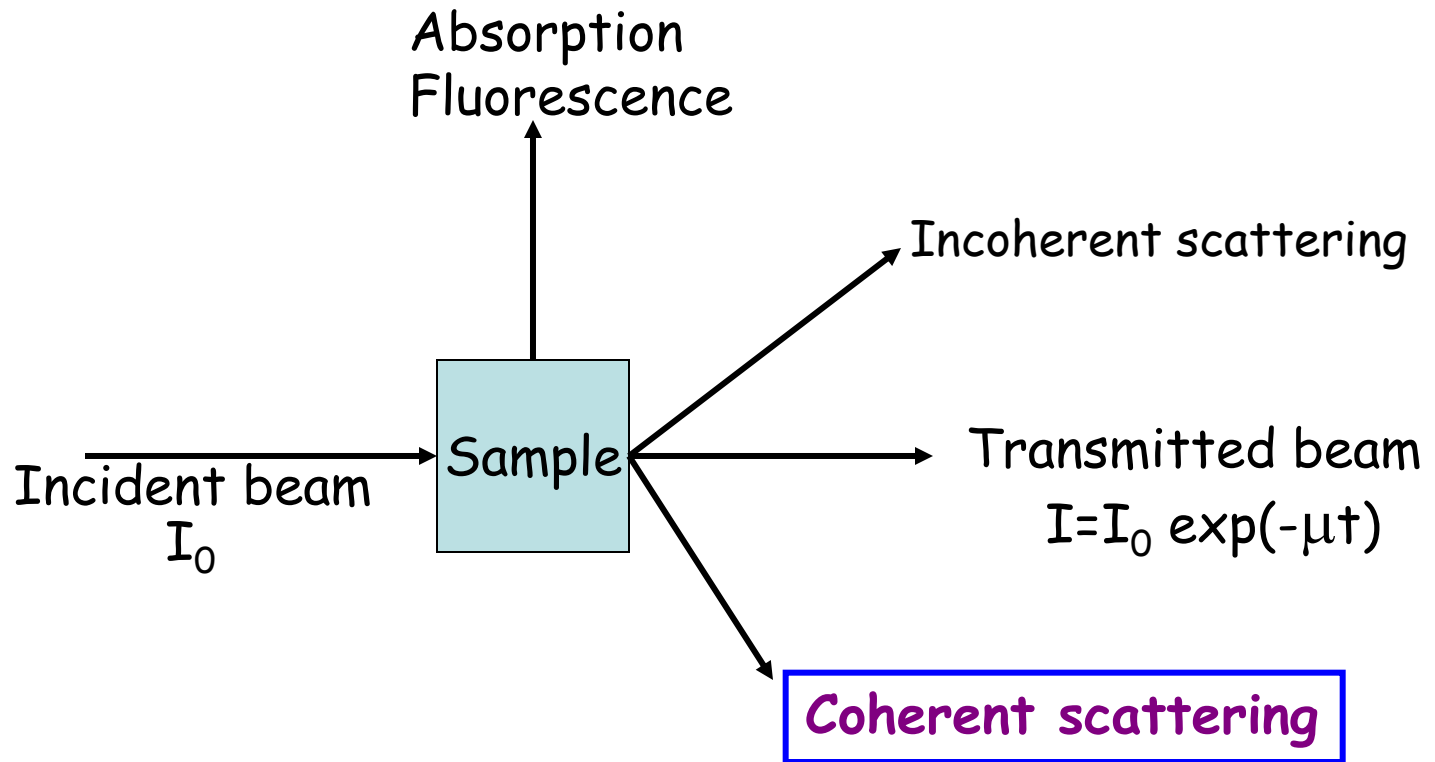
Determination of 3D solution structure at high resolution.

SAXS

Modeling of molecular shape envelope at low resolution.
Determination of structural parameters e.g. Radius of gyration (R_g), molecular mass (MM) etc.

Dynamic measurements to detect changes in structure upon a perturbation.

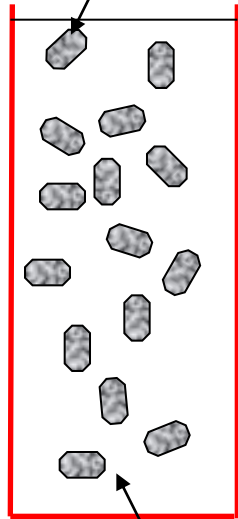
Interactions of X-Rays with Matter



- Coherent scattering; Structural information at the atomic/molecular level.
- Absorption, fluorescence, near edge measurements:
Material characterization, local structure, coordination.
- Transmission/phase contrast:
Lower resolution imaging.

Small Angle X-ray Scattering (SAXS)

Macromolecules



Buffer solution

Reciprocity law of scattering:

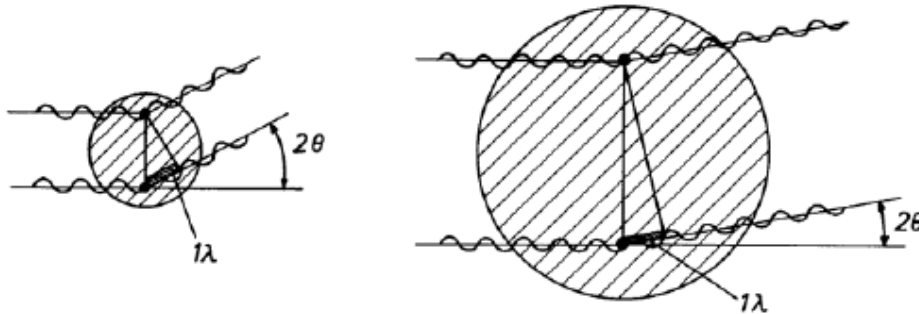
inverse relationship between particle size and scattering angle.

Dimensions of biological macromolecules (D_{\max}) \gg wavelength of X-rays (λ).

Scattering takes place at low angles.

Inhomogeneities in electron density in a solution of macromolecules in buffer \Rightarrow small angle X-ray scattering (coherent scattering).

Scattering Curves and Particle Size



Scattering angle 2θ .
Path difference 1λ .

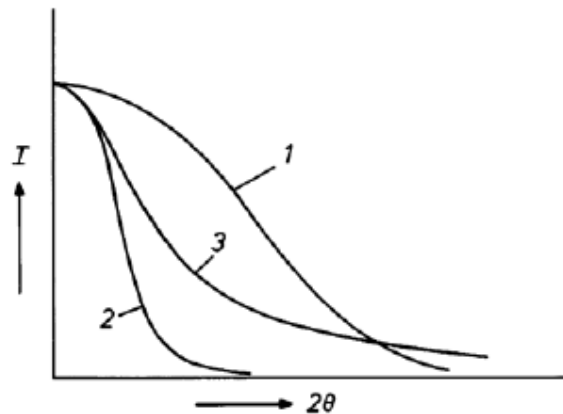
Destructive interference;
No scattering

Scattering angle $< 2\theta$
Scattering..

Scattering angle = 0
Maximum scattering. (Curve 1)

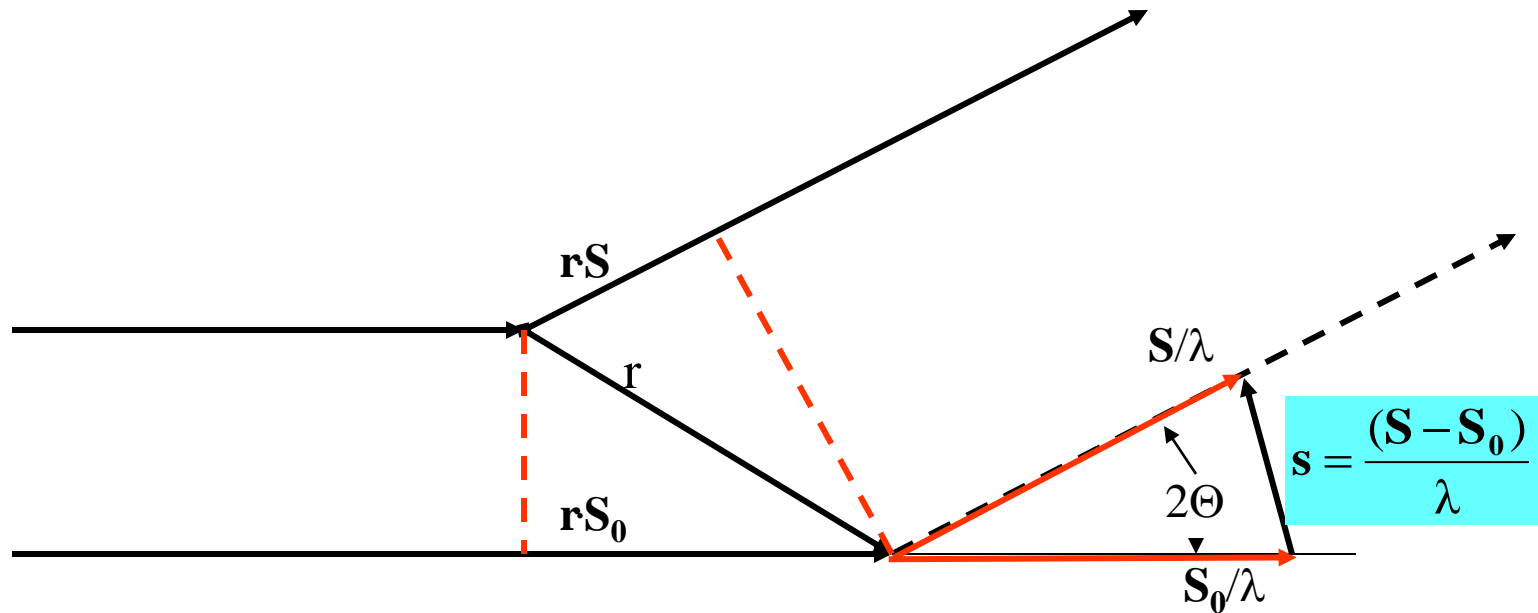
Effect of particle size:

Large particles
path difference 1λ occurs at
smaller angles (Curve 2).



Interference and Coherent Scattering

In coherent scattering the path length difference between waves scattered at different electrons is fixed and amplitudes are added.



Path difference = $\mathbf{r} \cdot \mathbf{S} - \mathbf{r} \cdot \mathbf{S}_0$

$$|\mathbf{s}| = \frac{2\sin\theta}{\lambda}$$

The total amplitude from two centers (one at the origin and one at \mathbf{r}) is:

$$F(\mathbf{s}) = \sum_{i=1}^2 f_e \exp(2\pi i \mathbf{s} \cdot \mathbf{r}_i) = f_e + f_e \exp(2\pi i \mathbf{s} \cdot \mathbf{r}_2)$$

Scattering from Crystals vs from Solutions

$$F(\mathbf{s}) = \sum_{i=1}^N f_i(\mathbf{s}) \exp(2\pi i \mathbf{s} \cdot \mathbf{r}_i)$$

“Structure factor”

Fourier transform of the distribution of the spherical atoms.

In SAXS $F(\mathbf{s})$ refers to structure of the solution; solvent + homogeneous distribution of proteins

The intensity:

$$I(\mathbf{s}) = \sum_{i=1}^N \sum_{j=1}^N f_i(\mathbf{s}) f_j(\mathbf{s}) \exp(2\pi i \mathbf{s} \cdot (\mathbf{r}_i - \mathbf{r}_j)) \longrightarrow \text{Crystal structure}$$

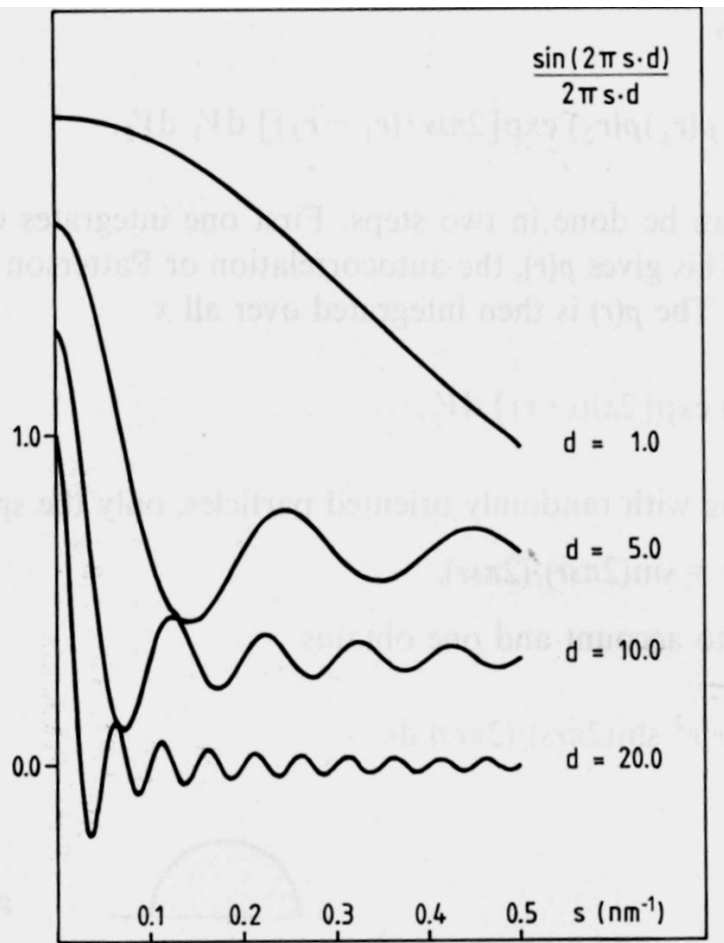
In solution particles are randomly oriented

$$\langle \exp(2\pi i \mathbf{s} \cdot (\mathbf{r}_i - \mathbf{r}_j)) \rangle = \frac{\sin(2\pi s r_{ij})}{2\pi s r_{ij}}$$

$$I(\mathbf{s}) = \sum_{i=1}^N \sum_{j=1}^N f_i(\mathbf{s}) f_j(\mathbf{s}) \frac{\sin(2\pi s r_{ij})}{2\pi s r_{ij}}$$

Contribution of r_{ij} to the Scattering Pattern

$$I(s) = \sum_{i=1}^N \sum_{j=1}^N f_i(s) f_j(s) \frac{\sin(2\pi s r_{ij})}{2\pi s r_{ij}}$$



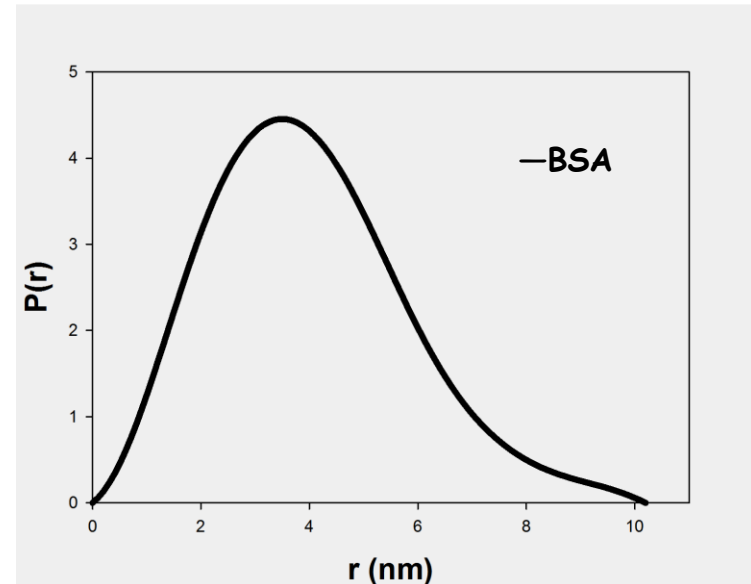
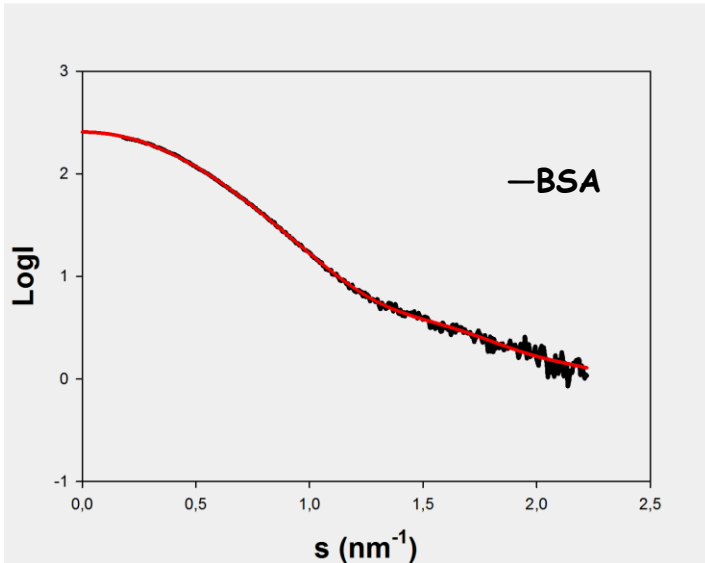
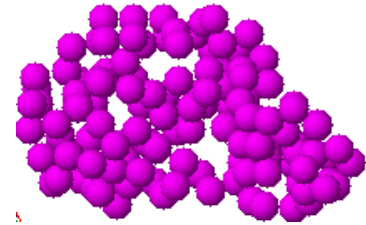
$$d = r_{ij}$$

Short distances; low frequencies dominate.

Large distances; high frequencies dominate higher angles.

I(s) and Distance Distribution Function P(r)

$$I(s) = 4\pi \int_0^{D_{\max}} p(r) \frac{\sin(2\pi sr)}{2\pi sr} dr$$

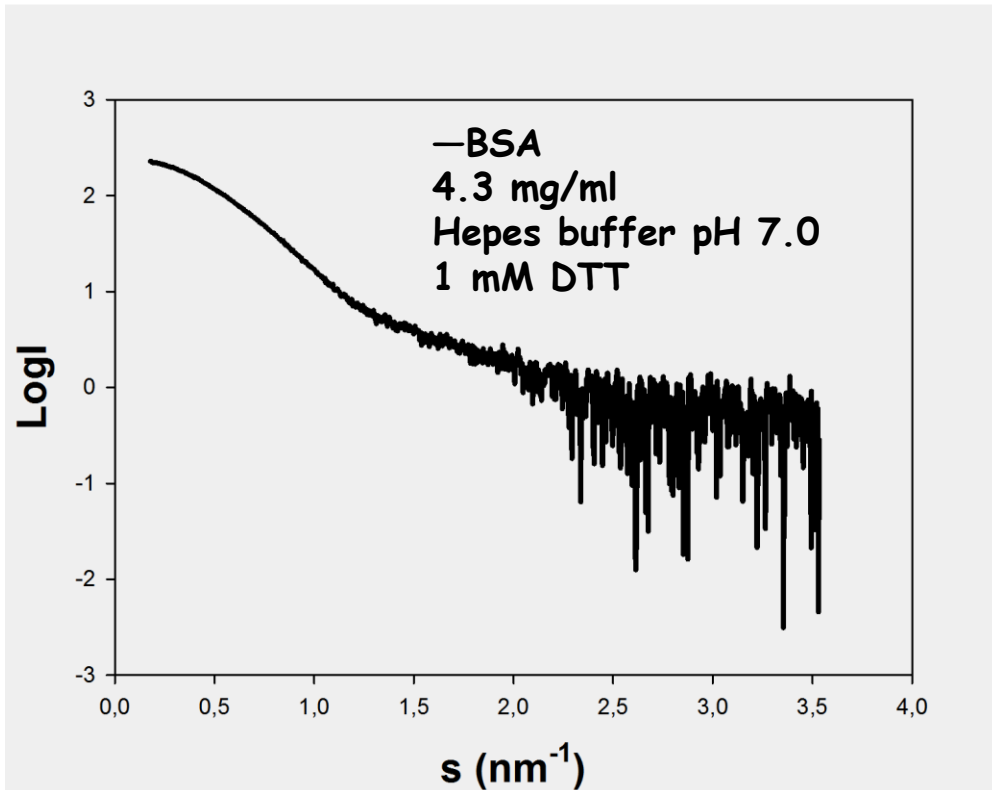


$$p(r) = 2r^2 \int_0^{\infty} I(s) \frac{\sin(2\pi sr)}{2\pi sr} ds$$

For a homogeneous particle $p(r)$: the histogram of distances between pairs of points within the particle.

Scattering intensity and $p(r)$ are related by a Henkel transformation.

Scattering Intensity

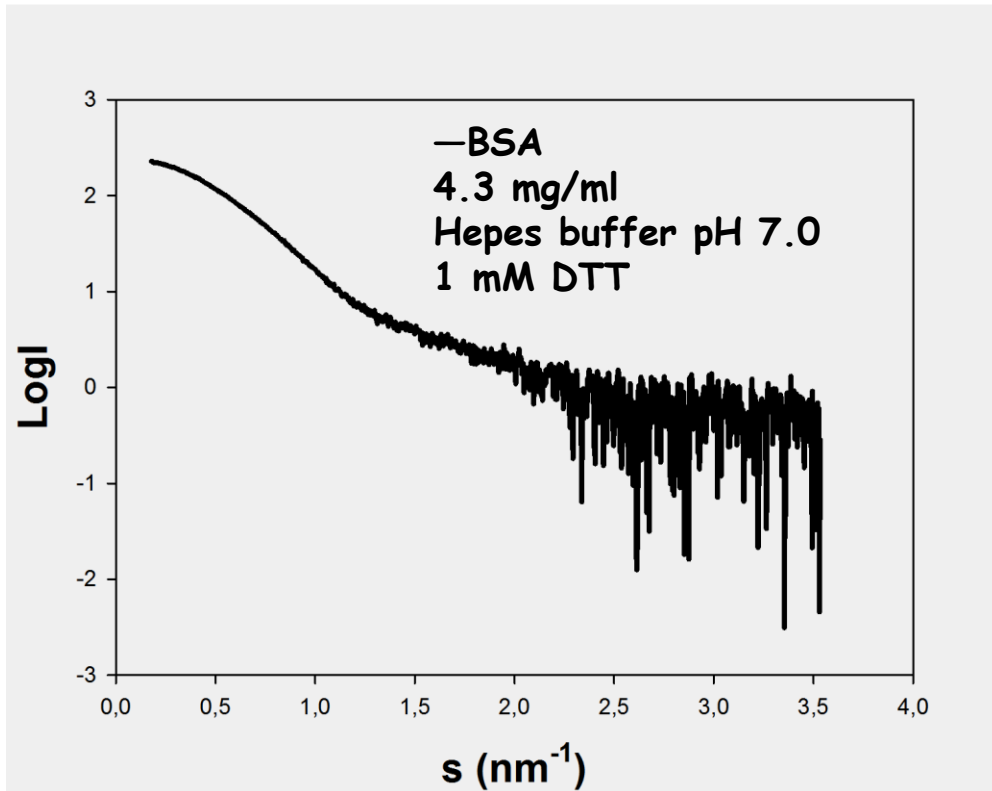


-Scattering intensity is the absolute square of the resultant amplitude.

-In contrast with a diffraction pattern it is a continuous function.

I(s) and Structural Parameters

I(s) is dependent on the molecular shape and size.



I(0) proportional to the **molecular mass (MM)** of protein. Determine with respect to protein with known MM.

Guinier approximation:

$$I(s) = I(0)\exp(-s^2R_g^2/3)$$

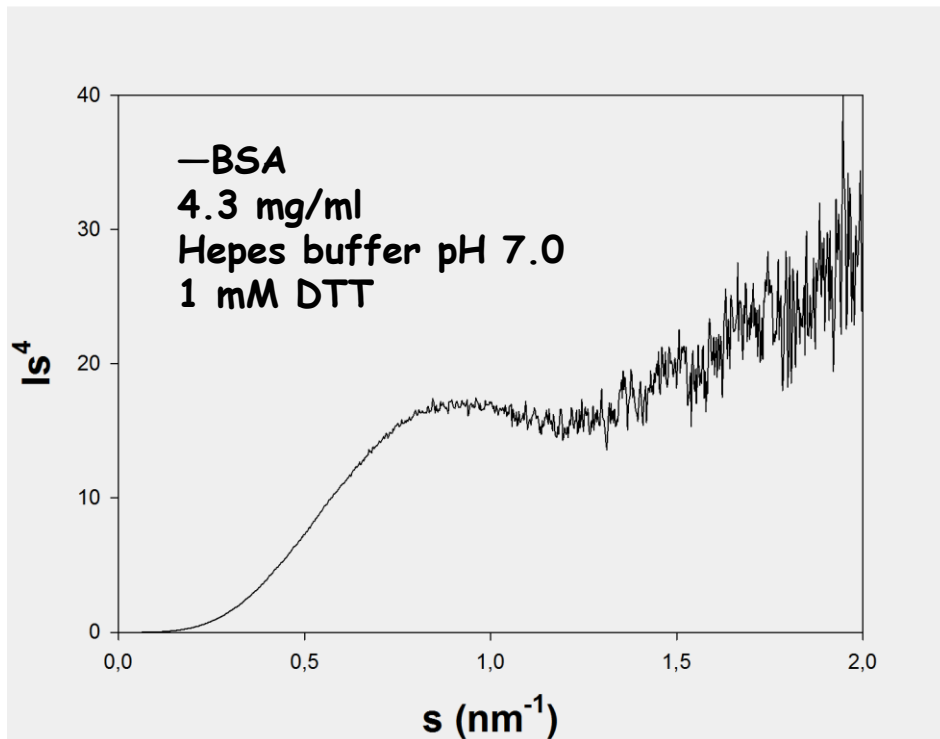
$$sR_g \lesssim 1.3$$

R_g is the **radius of gyration** for the particle.
Plot of $\ln I(s)$ vs s^2 .

I(s) and Structural Parameters

Porod Volume

$I(s)s^4$ vs s ; particle volume
supplementary information on molecular mass (MM).

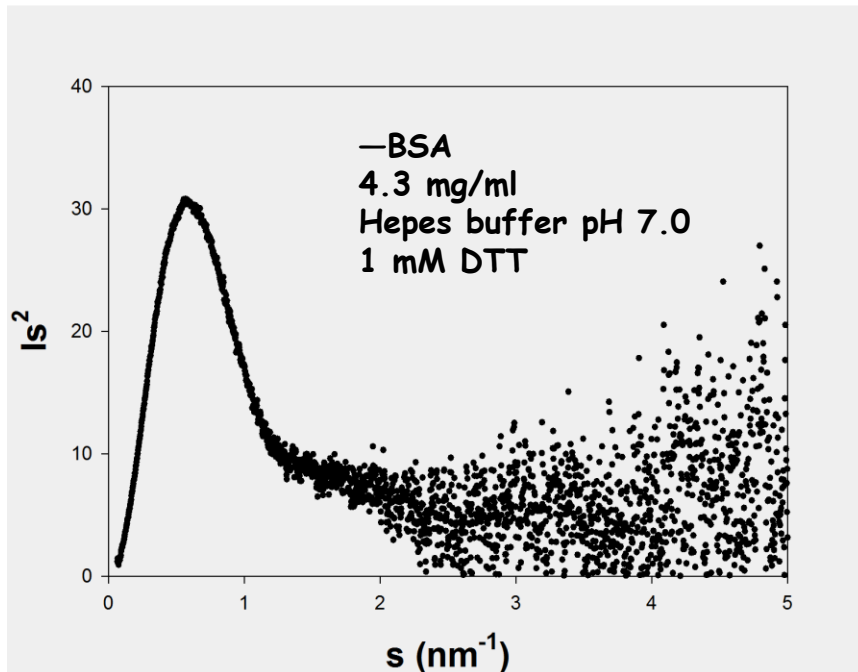


MM is estimated as
 $\frac{1}{2}$ Porod volume.

I(s) and Structural Parameters

Kratky Plot

$I(s)s^2$ vs s ; information on shape e.g. globular or extended
folded or natively unfolded, flexible or rigid
structure.

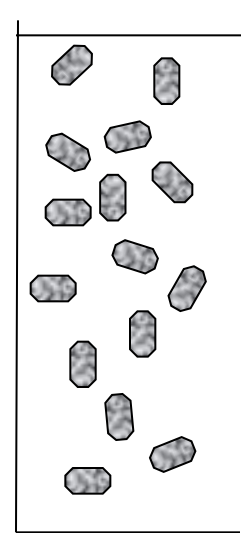


Unfolded proteins would display a monotonously increasing Kratky plot.

Contrast

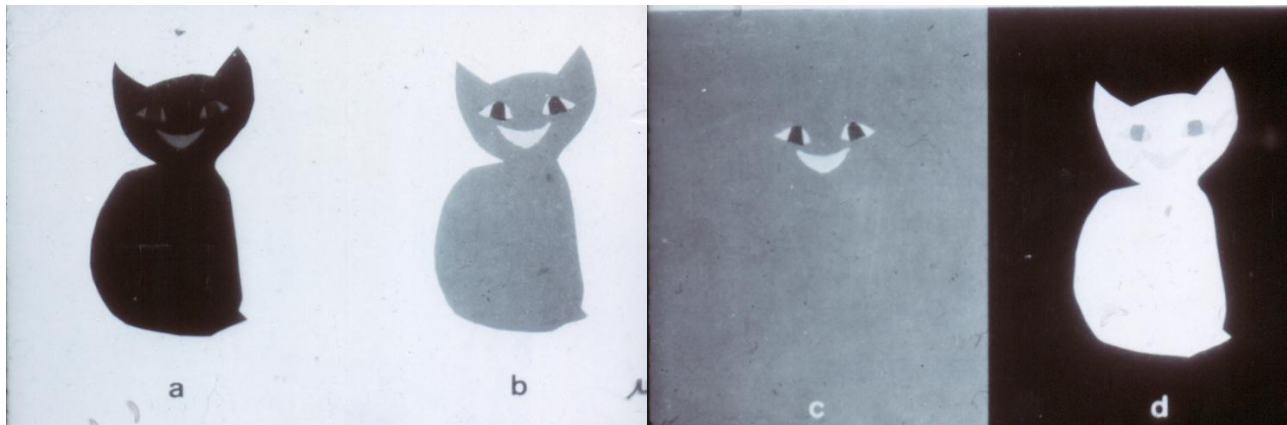
Particle:
$$F_p(\mathbf{s}) = \int_V \rho_p(\mathbf{r}) \exp(2\pi i \mathbf{s} \cdot \mathbf{r}) d\mathbf{r}$$

Solvent:
$$F_b(\mathbf{s}) = \rho_b \int_V \exp(2\pi i \mathbf{s} \cdot \mathbf{r}) d\mathbf{r}$$



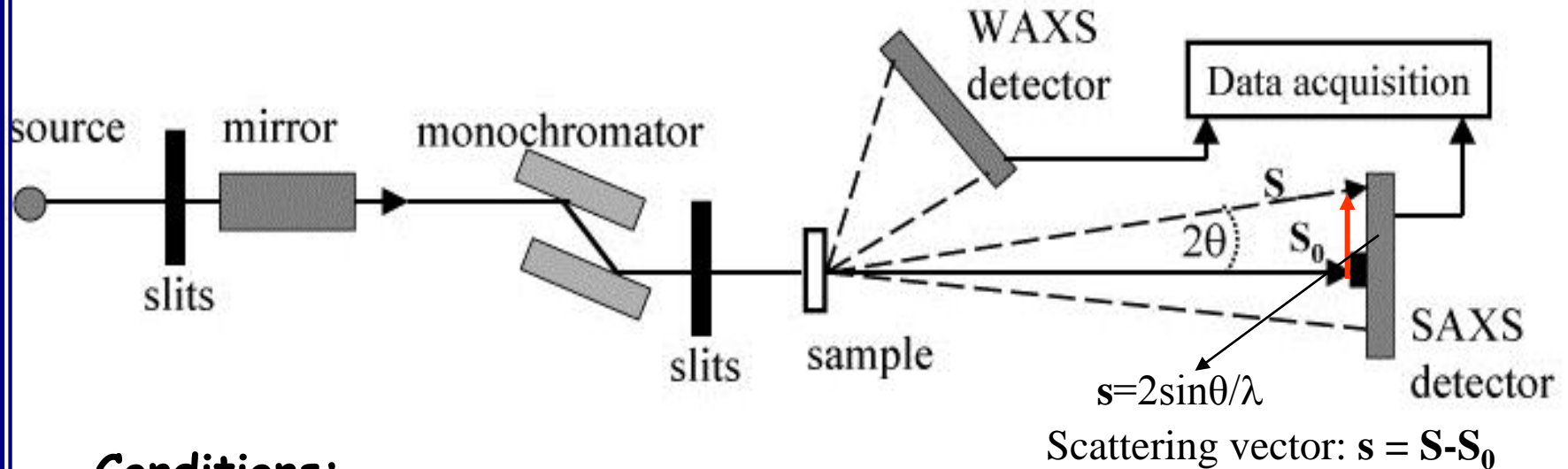
Only fluctuations in electron density contribute to the scattering:

$$I_{\text{obs}}(\mathbf{s}) = I_p(\mathbf{s}) - I_b(\mathbf{s})$$



“Contrast matching”

SAXS Beamline Basics



Conditions:

$$d \ll D$$

$$\Delta\lambda/\lambda \leq 0.1$$

$$\sin 2\theta = 2\theta$$

$$\cos 2\theta = 1$$

d : distance on the detector, D : Sample-Detector distance

WAXS: Wide angle X-ray Scattering

X33 Small angle X-ray scattering instrument of EMBL in HASYLAB.

X33 Beamline @ EMBL Hamburg Outstation

DORIS III/DESY 4.4 GeV, 120 mA.

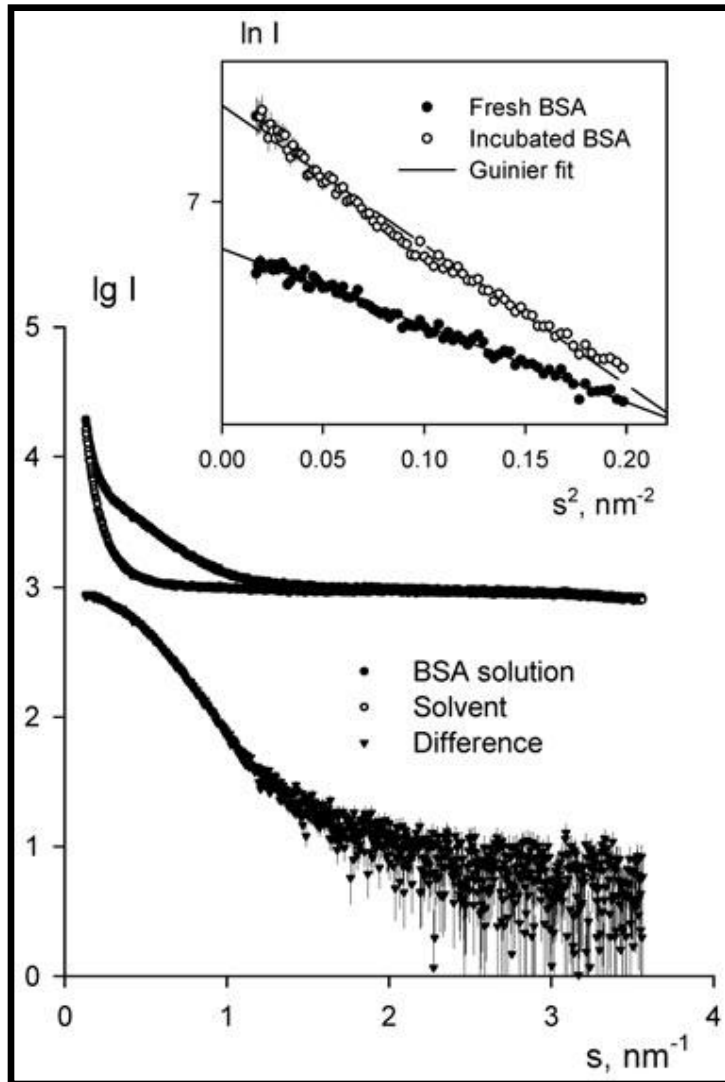


Automatic sample changer, sample can be kept under anaerobic conditions during measurements.

Marr/Pilatus detector, basic data reduction coupled to data collection.



Basics of SAXS Data Reduction



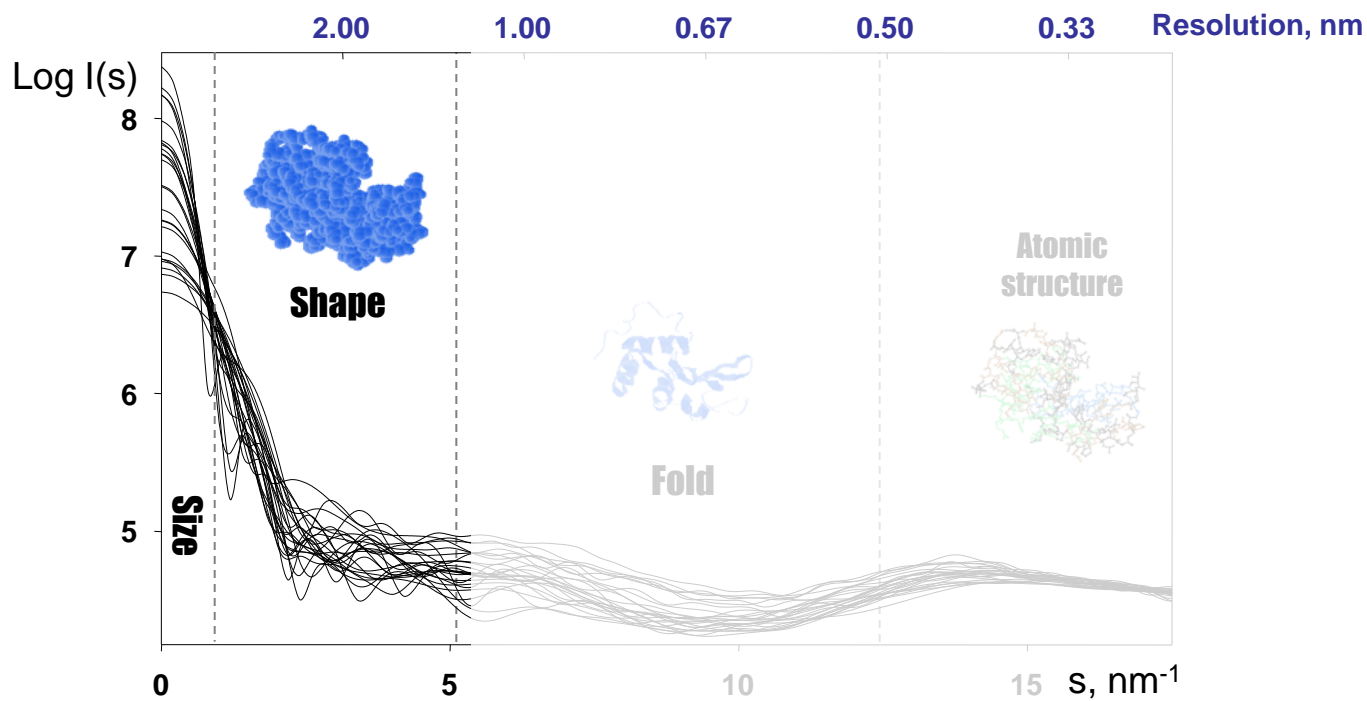
$$I(s) = \frac{1}{c} \left[\frac{I_s(s)}{I_{s,0}} - \frac{I_b(s)}{I_{b,0}} \right] \frac{1}{D(s)}$$

$I(s)$ scattered intensity,
 $I_s(s)$ scattering from the sample,
 $I_b(s)$ scattering from the buffer,
 C concentration of the sample,
 $I_{s,0}$ and $I_{b,0}$ through beam for sample
 and buffer respectively,
 $D(s)$ detector response.

Data quality:

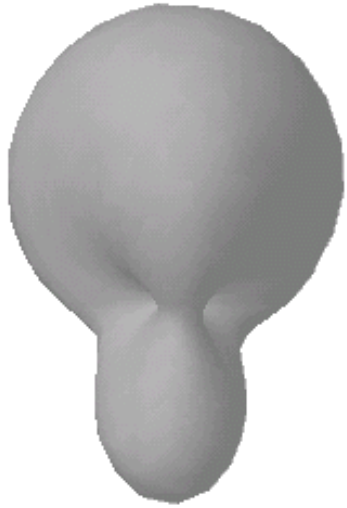
aggregation
 polydispersity
 improper background subtraction
 concentration correction

Analyzing SAXS Data



Ab initio Shape Determination

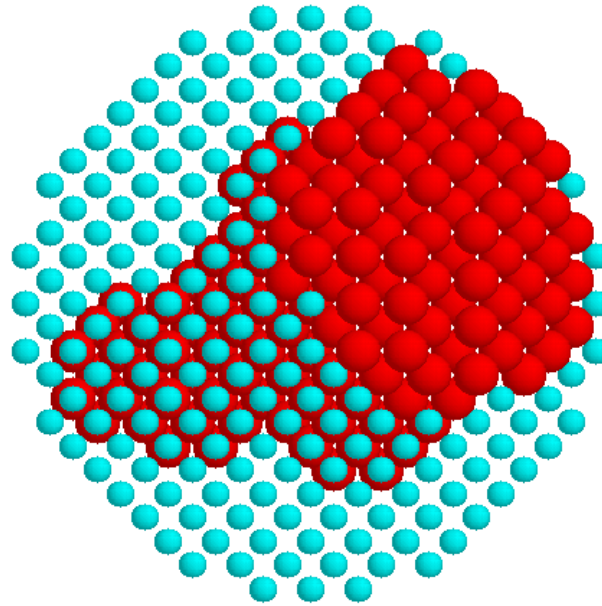
Low Resolution 3D Models



Envelope function

Stuhrmann, H. B. (1970) *Z. Physik. Chem. N.F.* **72**, 177

Svergun, D.I. *et al.* (1996) *Acta Crystallogr.* **A52**, 419

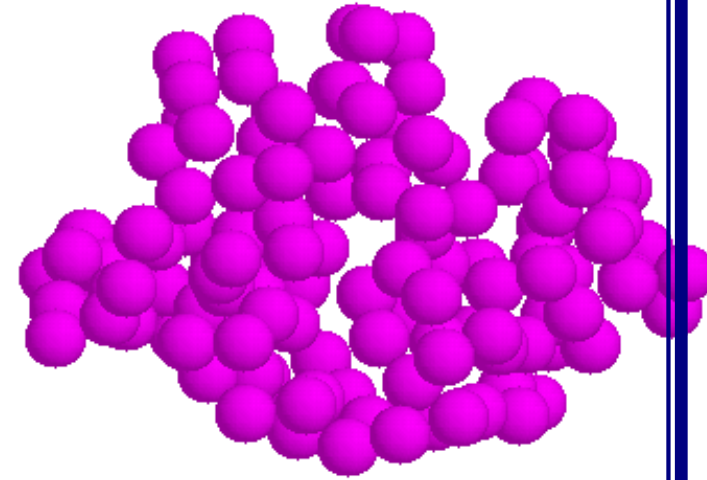


Dammin/Dammif

Bead models

Chacón, P. *et al.* (1998) *Biophys. J.* **74**, 2760

Svergun, D.I. (1999) *Biophys. J.* **76**, 2879



Gasbor

Dummy residues model

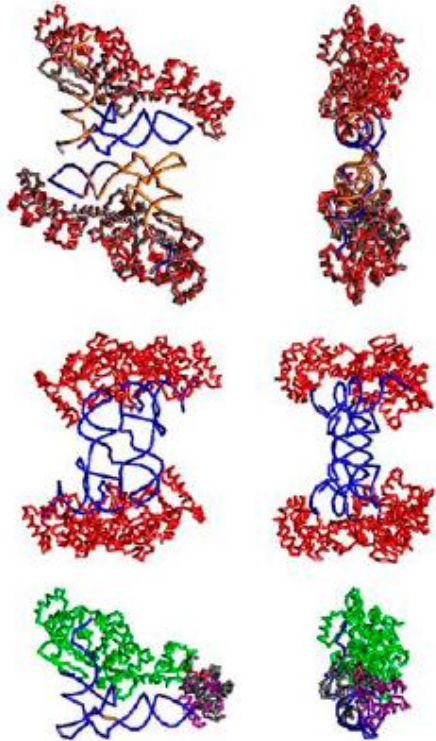
Svergun, D.I., Petoukhov, M.V. & Koch, M.H.J. (2001) *Biophys. J.* **80**, 2946-2953

These methods all minimize $\text{Discrepancy}[\text{Data}] + \text{Penalty}[\text{Additional info}]$

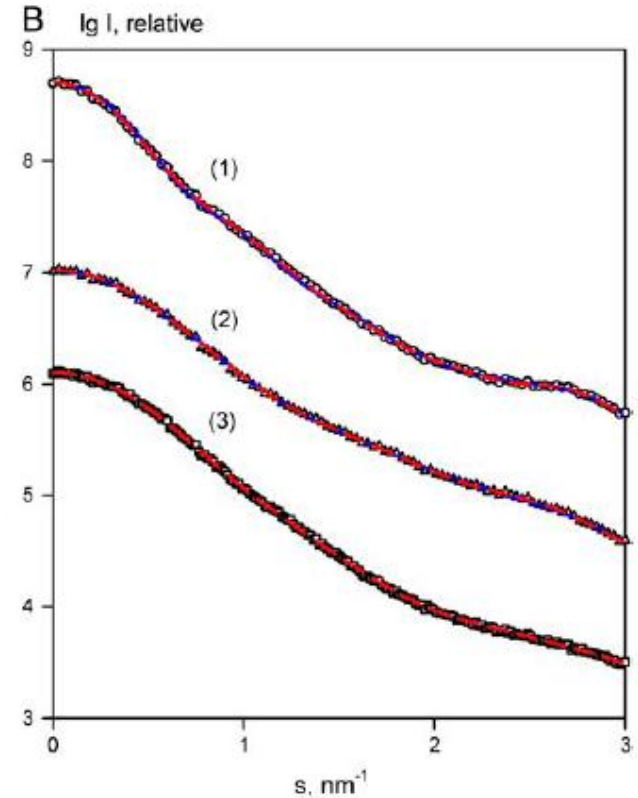
Oligomeric Forms and Missing Domains

Validation of modeling using simulated data from glutamyl-tRNA synthetase (GTS) complexed with tRNA (1g59)

A



B



SASREF for reconstructing oligomeric structures.
BUNCH for reconstructing with missing domains.

Petoukhov, M. V. And Svergun, D. (2005)

SAXS Based Information

Shape determination and low resolution structural analysis for bio-molecules that do not crystallize.

Combination with PX data from homologs to obtain structural information.

Combination with PX data to obtain structural information about missing domains.

Structural analyses of large complexes.

Investigation of intermediates during assembly.

Investigation of shape changes in response to perturbations.

SAXS Measurements with Plant Proteins

Abiotic stress responses in plants

Durum wheat metallothionein dMT

Small molecular weight ~7 kDa.
Does not crystallize.

Heterotrimeric G-protein subunits from *Arabidopsis thaliana*

Complex of three subunits molecular weight ~100 kD.
Modified forms from mammalian cells crystallize.

Large structural changes upon interactions. Studies in solution

Durum Wheat Metallothionein (dMT)



At 25 μM Cd.

-Metallothionein (*mt*) gene identified in durum wheat **tolerant to cadmium**. (Metal stress)

-Recombinant protein is produced in bacteria as fusion with *GST* (*GSTdMT*) for purification with and without *GST*, characterization and mutations.

dMT Amino acid sequence: 7 kDa

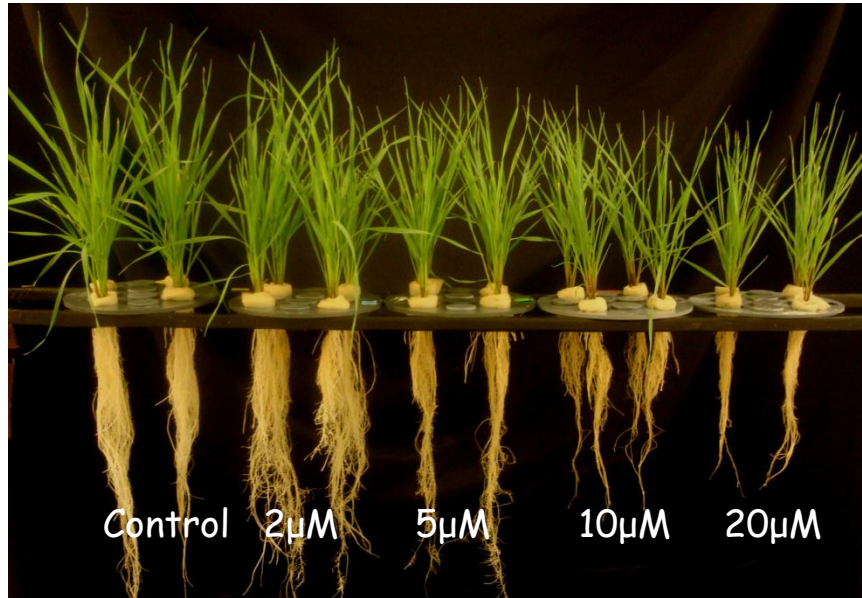
* * * * *
MSCNCGSGCSCGSDCKCGKMYPDLTEQGSAAAQVAAVVVLGVAPENKAGQFEVAAGQSGE* * * * *
GCSCGDNCKCNPCNC

**N-terminal
 β -domain**

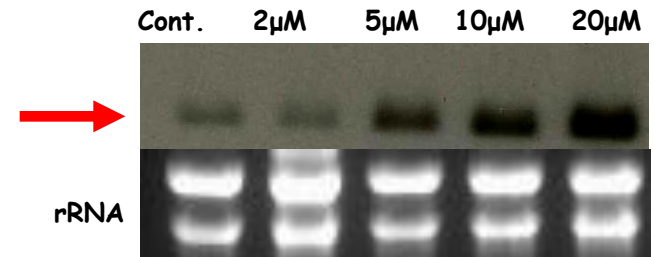
Hinge region

**C-terminal
 α -domain**

dMT Expression Under Cadmium Stress



Shoot and root growth of the durum wheat cultivar Balcalı-85 with increasing Cd application.



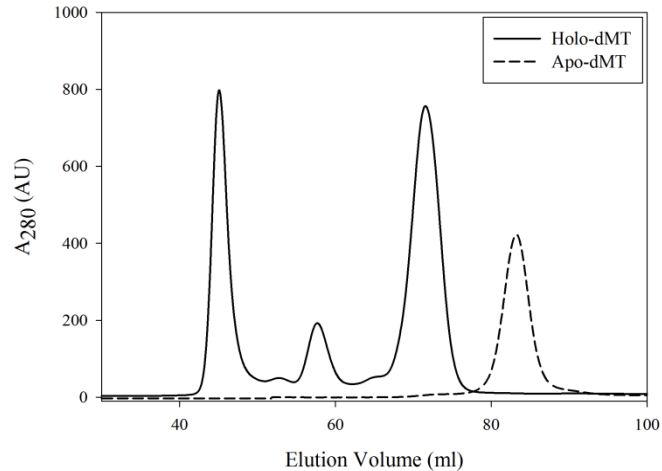
Northern blot analysis of Cd dose dependent expression of *dmt* gene in roots of *T. durum*.

dMT synthesis is induced during Cd-response

Bilecen et al 2005
Dede et al 2006
Yesilirmak and Sayers 2009
Aydin et al 201 (in preparation)

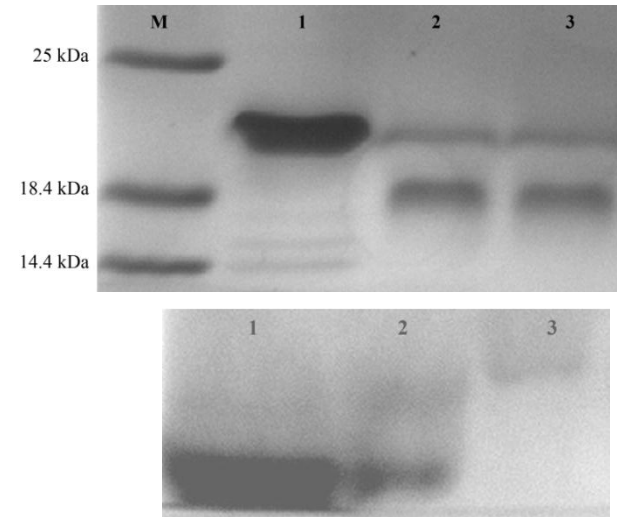
dMT Purification and Characterization

Size Exclusion Chromatography

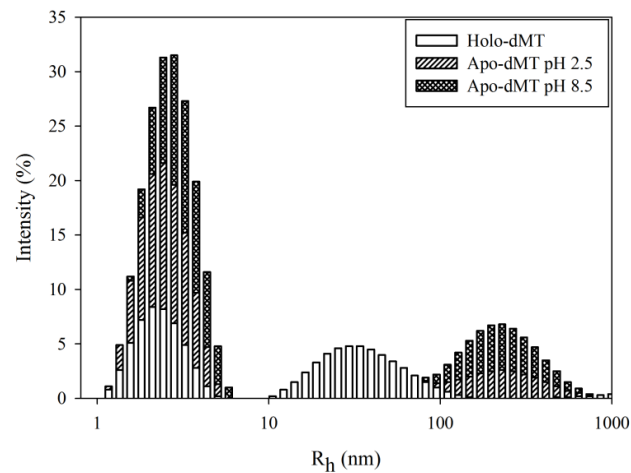


Holo-dMT: 10-16 kDa
Apo-dMT: 8-9 kDa

SDS- and Native-PAGE Analysis

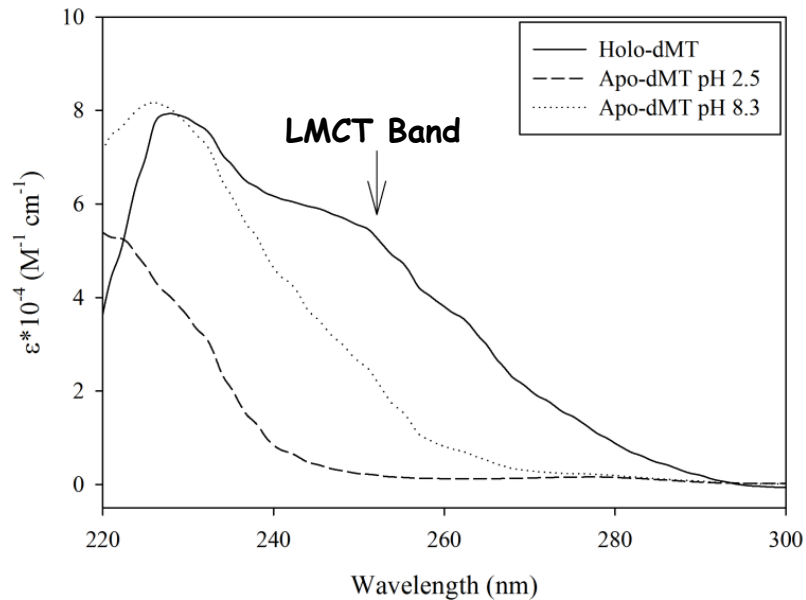


DLS Measurements

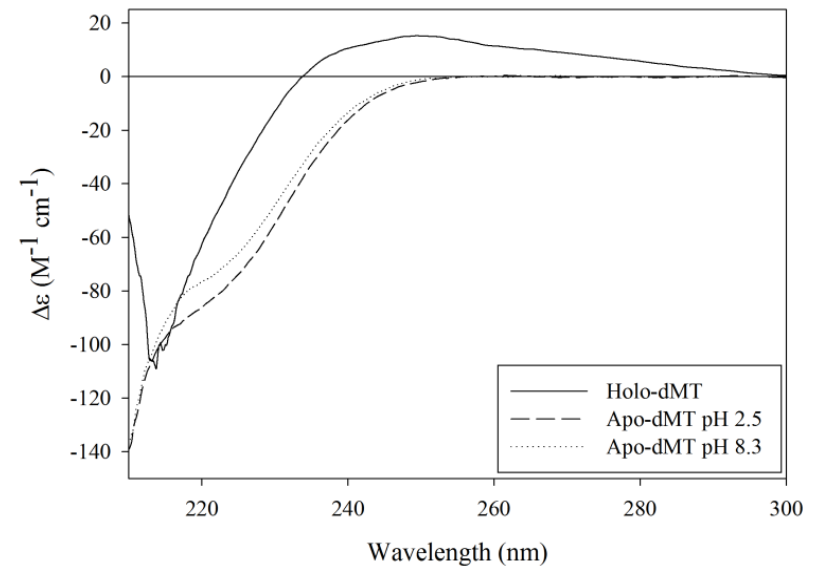


dMT Purification and Characterization

UV Absorbance Measurements



Circular Dichroism Spectropolarimetry Measurements

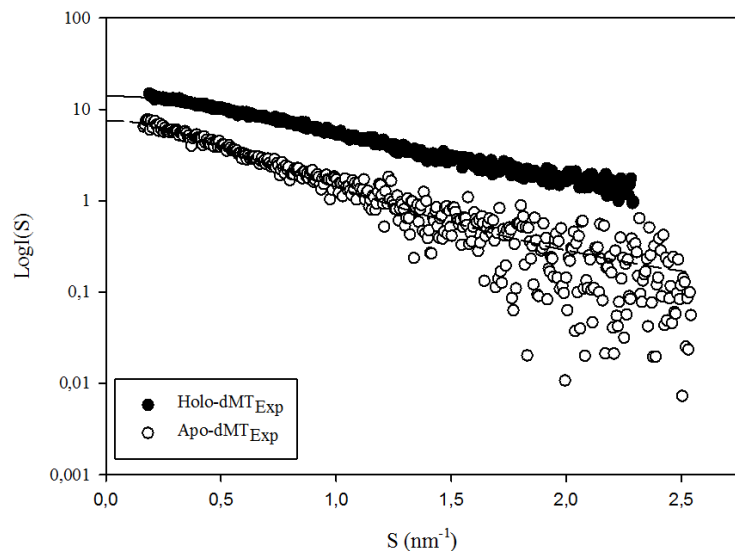


Cadmium Content (ICP-OES)

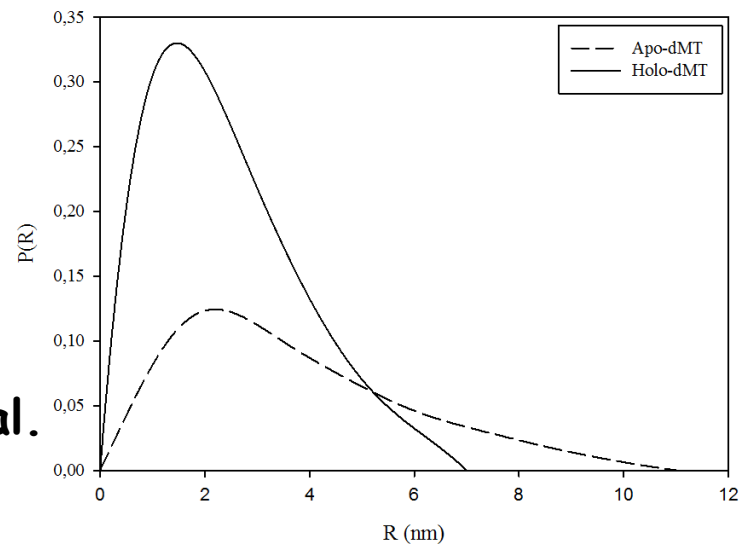
$5.3 \pm 0.5 \text{ Cd ions/dMT}$

Pushing SAXS to its Limits: Scattering from dMT

Scattered Intensity



P(R) Functions



E. Bal.

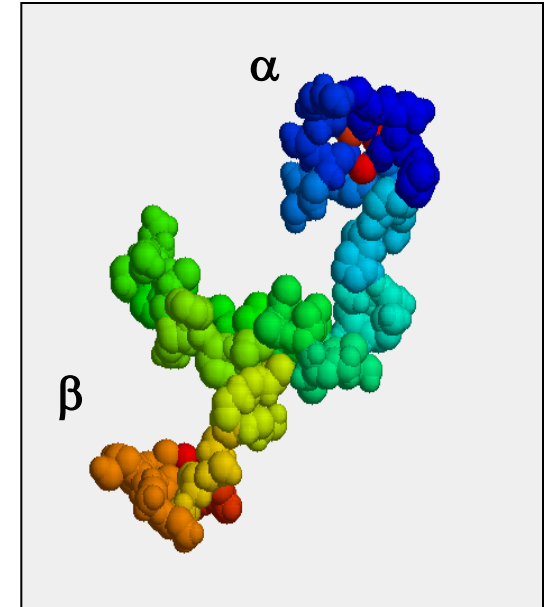
Structural Parameters

	Conc (μM)	R_g (nm)	D_{max} (nm)	$I(0)$	$\text{MM}_{\text{ex}}^{\text{p}}$ (kDa)	$\text{MM}_{\text{t}}^{\text{h}}$ (kDa)
Holo-dMT	192	2.10	7	14.25	17	16.9
Apo-dMT pH 2.5	174	2.98	11	7.6	9.1	7.89
Apo-dMT pH 8.3	174	2.66	8.9	6.8	8.1	7.89

Durum Wheat Metallothionein (dMT)

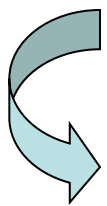
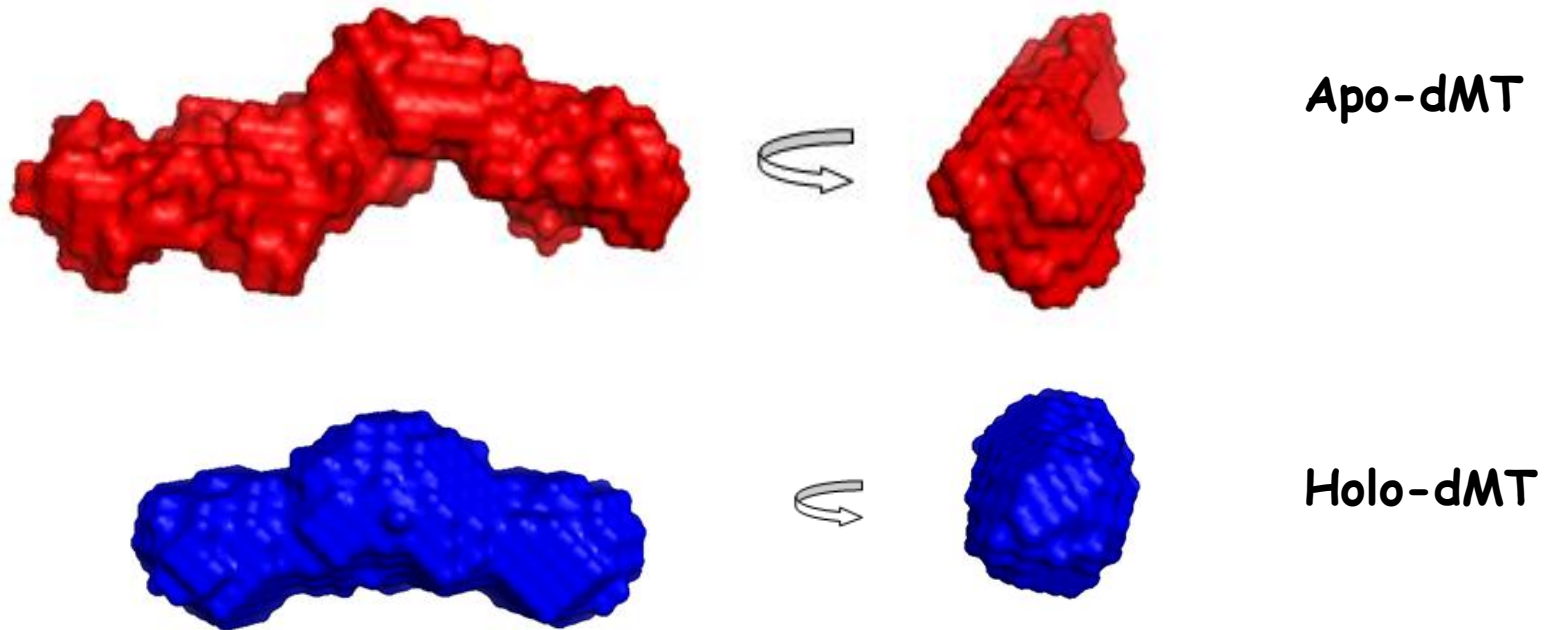
Homology modeling

Known homologs for metal-binding domains,
Ab initio for the hinge region



Elongated two domain structure with a folded hinge region

Ab initio Models of Apo- and Holo-dMT



Holo-dMT is stable as staggered dimer in the presence of Cd^{2+} . Oligomeric forms appear to be responsible for more efficient removal of toxic metals.

ACKNOWLEDGEMENTS



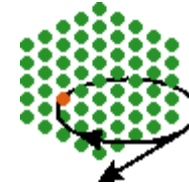
E. Bal, A. Akturk, M. Aydin
E. Mollamehmetoglu, T. Yenice
G. Dinler (ITU), F. Yesilirmak (IYTE), B. Kaplan (Lyon).
F. Kisaayak.
C. Saygi, and A. San.

SUPPORT

Supported by Turkey-Germany bilateral programs TBAG-U-155 and TBAG-U-157
Sabanci University Internal Research Fund IACF08-00514

Antalya 2010

COLLABORATORS



EMBL Hamburg

M.H.J. Koch
D. Svergun
M. V. Petoukhov
P. Konarev
M. Roessle
A. Kikhney
B. W. Shang
W. Meyer-Klaucke

Sabancı
Üniversitesi

U. Sezerman
I. Cakmak
H. Budak